PHYSICAL REVIEW A **93**, 041801(R) (2016)

Modulational instability and zigzagging of dissipative solitons induced by delayed feedback

D. Puzyrev,[1,2] A. G. Vladimirov,[1,3] S. V. Gurevich,[4,5] and S. Yanchuk[1,2]
[1]*Weierstrass Institute, Mohrenstrasse 39, D-10117 Berlin, Germany*
[2]*Institute of Mathematics, Technical University of Berlin, Strasse des 17 Juni 136, D-10623 Berlin, Germany*
[3]*Lobachevsky State University of Nizhni Novgorod, pr. Gagarina 23, Nizhni Novgorod, 603950, Russia*
[4]*Institute for Theoretical Physics, University of Münster, Wilhelm-Klemm-Strasse 9, D-48149 Münster, Germany*
[5]*Center for Nonlinear Science (CeNoS), University of Münster, Corrensstrasse 2, 48149 Münster, Germany*
(Received 27 October 2015; published 7 April 2016)

We report a destabilization mechanism of localized solutions in spatially extended systems which is induced by delayed feedback. Considering a model of a wide-aperture laser with a saturable absorber and delayed optical feedback, we demonstrate the appearance of multiple coexistent laser cavity solitons. We show that at large delays apart from the drift and phase instabilities the soliton can exhibit a delay-induced modulational instability associated with the translational neutral mode. The combination of drift and modulational instabilities produces a zigzagging motion of the solitons, which are either periodic, with the period close to the delay time, or chaotic, with low-frequency fluctuations in the direction of the soliton motion. The same type of modulational instability is demonstrated for localized solutions of the cubic-quintic complex Ginzburg-Landau equation.

DOI: 10.1103/PhysRevA.93.041801

The formation and complex dynamics of localized patterns in dissipative systems have been reported in different areas of research. They manifest themselves as localized light spots in nonlinear optics [1–5], solitary waves in fluid dynamics [6,7], concentration pulses or spots in chemical and biological systems [5,8,9], current filaments in semiconductor devices and gas-discharge systems [10–12]. In this Rapid Communication, we focus on the effects of the delayed feedback on the dynamical properties of localized structures. One of the established examples of localized structures are cavity solitons (CSs), which are localized spots of light in the transverse section of passive and active optical devices, broad area lasers and wide-aperture semiconductor cavities with external coherent pumping [1,13]. Recently, much attention was paid to the investigation of the influence of the delayed optical feedback on the stability properties of these structures [14–16]. In particular, it was demonstrated that in a driven passive cavity with delayed feedback a drift instability of a cavity soliton leading to a motion in the transverse direction and some other instabilities can develop [14,15]. The influence of the feedback phase and carrier relaxation rate on the drift instability threshold was investigated in [16]. In this Rapid Communication, we show how the delayed optical feedback produces multistability of laser cavity solitons. Moreover, we describe a type of delay-induced modulational instability, which leads to zigzagging and drifting CSs, as well as a low-frequency switching of the soliton motions. We also show that the same modulational instability occurs for localized solutions of the cubic-quintic complex Ginzburg-Landau equation (CGLE) [17]. Since the CGLE plays a role of the normal form for a large class of complex spatially extended systems of different physical origin [18], our results are also relevant beyond the scope of nonlinear optics.

The dynamics of a wide-aperture laser with a saturable absorber subject to a coherent optical delayed feedback can be described by the one-dimensional quasioptical equation [19] with an additional delayed feedback term:

$$\partial_t A = (d+i)\partial_{xx} A + f(|A|^2)A + \eta e^{i\varphi} A(x,t-\tau), \quad (1)$$

where $A(t,x)$ is the slowly varying amplitude of the electric field; τ,η, and φ are delay time, feedback strength, and phase, respectively. Here, time t and transverse coordinate x are dimensionless, whereas $d\partial_{xx}A$ denotes a small diffusion term with a positive diffusion coefficient d. The delayed feedback term in Eq. (1) is introduced with the assumption that the external cavity is self-imaging, so that the diffraction in this cavity can be neglected [16]. Here, we focus on the case of instantaneous gain and absorption relaxation. Then the nonlinear function in Eq. (1) describing the saturable gain and absorption as well as linear cavity losses can be written in the form [20]

$$f(|A|^2) = -1 + \frac{g_0}{1+|A|^2/s} - \frac{a_0}{1+|A|^2}, \quad (2)$$

where g_0 and a_0 are linear gain and the absorption coefficients, and s is the ratio of the saturation intensities in the amplifying and absorbing media.

The CS solutions can be found in the form $A(x,t) = A_0(x)e^{-i\omega t}$, where $A_0(x)$ is the complex amplitude with the field intensity $|A_0|^2$ localized around some point in space and ω is the soliton frequency shift. The properties of localized solutions of Eq. (1) without delayed feedback ($\eta = 0$) were studied previously in detail, see, e.g., [20–22]. To find the localized solutions in the system with delayed feedback, we substitute the ansatz $A_0(x)e^{-i\omega t}$ into Eq. (1) and obtain the following ordinary differential equation for unknowns A_0 and ω:

$$(d+i)\partial_{xx}A_0 + i\omega A_0 + f(|A_0|^2)A_0 + \eta e^{i\theta} A_0 = 0. \quad (3)$$

Here $\theta = (\omega\tau + \varphi) \mod 2\pi$ denotes the effective feedback phase. Equation (3) defines a set of soliton solutions parametrized by the phase θ. This set can be calculated in a similar way as in the system without delay, since Eq. (3) is an ordinary differential equation. In this way, one can find ω_θ and $A_{0,\theta}(x)$. Then the solitons within this set corresponding to any given value of time delay τ are determined from the condition

$$\omega_\theta \tau + \varphi = \theta \mod 2\pi. \quad (4)$$

As soon as the dependency ω_θ is calculated numerically, the solutions θ_k of Eq. (4) define the cavity soliton solutions with the frequencies ω_{θ_k} at a given value of time delay τ. Therefore, as a first step it is necessary to describe the whole set of solitons in Eq. (3) for all possible values of parameter θ.

It is known for the case with $\eta = 0$ [20] that the branch of CSs has a form of a spiral in the (g_0,ω) plane (green line in Fig. 1). Therefore, in a system perturbed by the delayed feedback $\eta > 0$, an offset spiraling branch of solitons appears in the (g_0,ω) plane for each fixed value of the effective feedback phase θ. The set of such branches for all possible θ forms a one-parametric family in the form of a spiraling tube with a diameter proportional to η (see Fig. 1).

For any given value of delay τ, the CSs can be found from relation (4), which defines a line on the tube. Figure 1 (black solid line) shows the resulting soliton branch for the feedback time $\tau = 250$. One can observe that the soliton branch makes a number of turns around the tube giving rise to multistability of CSs. Indeed, at the fixed value of the pump parameter g_0 and sufficiently large delay time τ, one obtains a set of external cavity solitons, similar to the case of external CW cavity modes in a single-mode laser with delayed feedback [23–29], cf. an inset in Fig. 1 where a cross-section of the tube is presented. There, black dots depict CS solutions for $\tau = 1000$ in the (P,ω) plane, where $P = \int dx|A_0|^2$.

A similar multistability effect was experimentally observed in a broad-area VCSEL (vertical cavity surface emitting laser) with frequency-selective feedback [30,31]. The existence of such a multistability follows from the form of Eq. (4), which can be rewritten as $\omega_\theta = (\theta - \varphi)/\tau + 2\pi k/\tau$. Properties of its solutions can be easily studied, e.g., geometrically. In particular, one can show that the number of solutions θ_k of this equation grows linearly with τ, and for large delay,

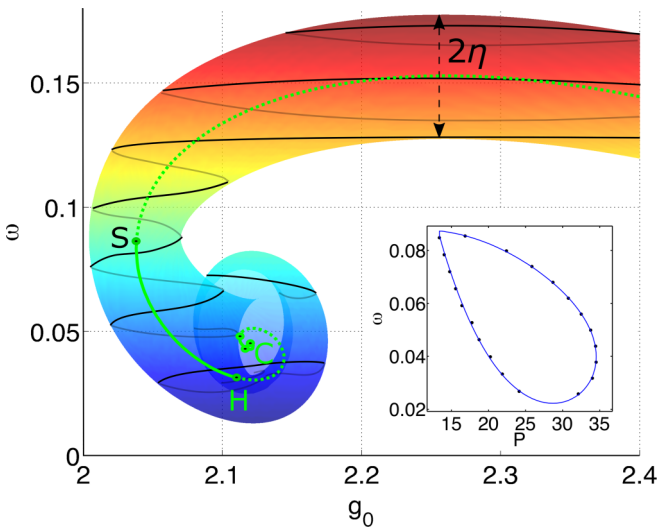

FIG. 1. Tube of solitons defined by Eq. (3) for all possible values of phase θ and other parameters fixed as $\eta = 0.025, \varphi = 0, a_0 = 2.0, I_g = 10.0$, and $d = 0.1$. The tube corresponds to all possible values of the delay time τ. Black line: soliton branch for $\tau = 250$. Green (light gray) line: branch of solitons for the case without feedback, $\eta = 0$ (solid for stable and dashed for unstable). **S** indicates a saddle-node bifurcation, and **H** an Andronov-Hopf bifurcation. The branch has the form of a spiral with the accumulation point **C**.

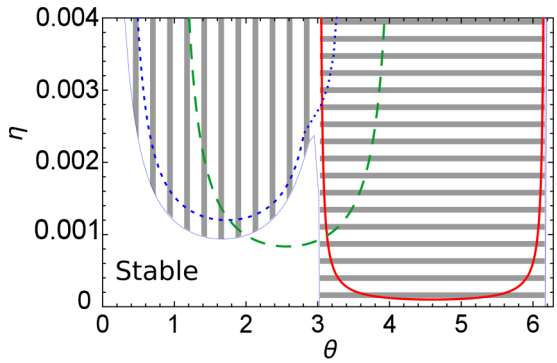

FIG. 2. Cavity soliton bifurcation diagram in (θ,η) plane. In the large delay limit, the horizontally hatched region corresponds to drift destabilization and the vertically hatched region to modulational instability related to the translational neutral mode. Solid red, dotted blue, and dashed green lines show the destabilization threshold for drift, modulational, and phase instabilities, respectively, calculated for $\tau = 1000$. Control parameter $g_0 = 2.07$.

the solutions cover the whole range of the phases θ with the spacing between them of the order $1/\tau$, cf. [27,29]. In particular, in the limit of large delay, the CS solutions densely fill the whole surface of the tube.

To analyze the stability of the localized solutions in the presence of delayed feedback, we apply the ansatz $A(x,t) = [A_0(x) + A_p(x,t)]e^{-i\omega t}$ in the evolution equation (1). Here, A_p stands for a small perturbation of the soliton solution. After linearization in A_p, we obtain

$$\begin{aligned}\partial_t A_p = &-i\omega A_p + (d+i)\partial_{xx}A_p \\ &+ f(|A_0|^2)A_p + |A_0|^2 f'(|A_0|^2)A_p \\ &+ {A_0}^2 f'(|A_0|^2)\overline{A_p} + \eta e^{i\theta}A_p(t-\tau). \qquad (5)\end{aligned}$$

By substituting $A_p(x,t) = [A_R(x) + iA_I(x)]e^{\lambda t}$ into Eq. (5), where λ is the complex eigenvalue, we arrive at the transcendental eigenvalue problem

$$L\Psi := [\tilde{L} - I\lambda + \eta B e^{-\lambda\tau}]\Psi = 0, \qquad (6)$$

where $\Psi = (A_R, A_I)^T$ is an eigenfunction, $\tilde{L}$ is the linearization of the instantaneous part, and B is a 2×2 matrix of rotation by angle θ. To find the eigenvalues numerically, we rewrite the eigenvalue problem (6) in matrix form by discretizing the space. The characteristic roots of the resulting system are found using the spectral method described in [32], see Fig. 3. With the increase of delay time τ, the computational complexity of the eigenvalue problem increases. However, as shown below, in such a case, the stability analysis can be significantly simplified by using a large delay approximation.

Drift bifurcation. Due to translational and phase-shift symmetries of Eq. (1), the operator L has two zero eigenvalues corresponding to a pair of eigenfunctions (also known as Goldstone modes) [22]: the even phase-shift neutral mode $\Psi^{\rm ph} = [-{\rm Im}A_0(x), {\rm Re}A_0(x)]^T$ and the odd translational neutral mode $\Psi^{\rm tr} = \partial_x[{\rm Re}A_0(x), {\rm Im}A_0(x)]^T$. The real eigenvalue which corresponds to Galilean symmetry [1-7] is generally nonzero due to diffusion and delayed feedback. Drift bifurcation occurs when the eigenvalue corresponding to the translational mode becomes doubly degenerate with geometrical multiplicity

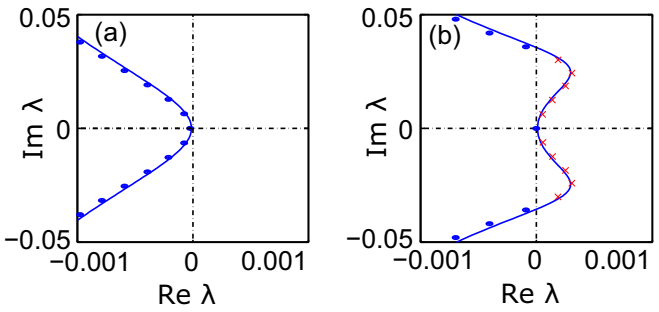

FIG. 3. Pseudocontinuous spectrum curves for $\eta = 0.005$. Stable soliton (a) for $\theta = 4$ and modulationally unstable soliton (b) for $\theta = 1.5$. Blue dots and red crosses show stable and unstable eigenvalues for $\tau = 1000$.

one [33]. That is, the critical real eigenvalue passes through zero at the bifurcation point, so that the corresponding critical eigenfunction at this point is proportional to $\Psi^{\rm tr}$. This critical eigenvalue can be either a delay-induced branch of zero translational eigenvalue or correspond to a Galilean mode. To determine the drift instability threshold let us look for real solutions of the eigenvalue problem (6) in the vicinity of zero, $\lambda = \varepsilon \ll 1$. The corresponding eigenfunction Ψ can be represented as $\Psi = \Psi^{\rm tr} + \varepsilon\Psi_1 + O(\varepsilon^2)$ with some unknown function Ψ_1. Substituting this expansion into Eq. (6), expanding the resulting equation into power series in ε, and collecting zero-order terms we get the relation $L_0\Psi^{\rm tr} = 0$ with $L_0 = \tilde{L} + \eta B$, which is satisfied by the definition of the neutral mode $\Psi^{\rm tr}$. Then, collecting the first-order terms in ε we obtain $L_0\Psi_1 = (I + \eta\tau B)\Psi^{\rm tr}$. This equation possesses a nontrivial solution if and only if the solvability condition is fulfilled which requires the orthogonality of the right-hand side to the translational eigenfunction $\Psi^{\rm tr\dagger}$ of the adjoint operator $L_0^\dagger$. The solvability condition leads to the expression

$$\eta_d = -p/[\tau(p\cos\theta - q\sin\theta)] \tag{7}$$

for the threshold feedback rate associated with the drift instability of the cavity soliton. Here $p = \langle\Psi_R^{\rm tr},\Psi_R^{\rm tr\dagger}\rangle + \langle\Psi_I^{\rm tr},\Psi_I^{\rm tr\dagger}\rangle$ and $q = \langle\Psi_I^{\rm tr},\Psi_R^{\rm tr\dagger}\rangle - \langle\Psi_R^{\rm tr},\Psi_I^{\rm tr\dagger}\rangle$, where $\Psi = (\Psi_R^{\rm tr},\Psi_I^{\rm tr})^T$ $[\Psi^{\rm tr\dagger} = (\Psi_R^{\rm tr\dagger},\Psi_I^{\rm tr\dagger})^T]$ is the translational neutral mode of L_0 (adjoint operator $L_0^\dagger$) and $\langle\Psi_j,\Phi_k^\dagger\rangle = \int_{-\infty}^{\infty}\Psi_j\Phi_k^\dagger dx$ [34].

When increasing the feedback rate above the threshold given by Eq. (7), a pitchfork bifurcation takes place: the stationary soliton loses stability, giving rise to a pair of branches of stable cavity solitons moving uniformly along the x axis in opposite directions. Note that the drift instability exists only in the interval of feedback phases θ, where the right-hand side in Eq. (7) is positive. The drift instability threshold calculated for $\tau = 1000$ is shown by the solid red line in Fig. 2. The domain where drift instability is possible for an arbitrary delay time is indicated by horizontal hatching.

Saddle-node phase bifurcation. Similar to the translational zero eigenvalue, the zero eigenvalue of the phase-shift neutral mode can become doubly degenerate in the presence of delayed feedback. The threshold of this instability η_p is given by Eq. (7) with the neutral modes $\Psi^{\rm tr}$ and $\Psi^{\rm tr\dagger}$ replaced by the phase-shift neutral modes $\Psi^{\rm ph}$ and $\Psi^{\rm ph\dagger}$ in the expressions for the coefficients p and q. In Fig. 2 it is shown by a dashed green line. In fact, this bifurcation corresponds to a saddle-node bifurcation, where a pair of soliton solutions merge and disappear (cf. Fig. 1), and it is defined by the condition $d\omega/d\theta = 1/\tau$, which follows directly from Eq. (4). By differentiating Eq. (3) by θ, one can easily show that this condition is equivalent to the condition $\eta = \eta_p$ obtained from Eq. (7) with the translational neutral mode replaced by the phase one. That is, the aforementioned multistability of the CSs is induced by the saddle-node phase bifurcation.

Modulational instability. It was shown in Refs. [35–37] that the spectrum of the delay systems is split into discrete and pseudocontinuous parts in the case when the delay time is sufficiently large to induce multiple delay-induced linear modes. While the aforementioned drift instability is associated with the discrete part of the spectrum, an instability of the pseudocontinuous part can produce another type of bifurcation scenario. Figure 3 shows a set of eigenvalues belonging to a branch of a pseudocontinuous spectrum with the translational zero eigenvalue at the origin. Figures 3(a) and 3(b) correspond to weakly stable and unstable cases, respectively, indicating the presence of delay-induced modulational instability [38]. The modulational instability is characterized by a branch of eigenvalues whose second derivative becomes positive in the origin as in Fig. 3(b).

To obtain the conditions for the onset of a modulational instability, let us consider the pair of complex-conjugate eigenvalues $\lambda_\pm$ with the smallest nonzero imaginary parts on the pseudocontinuous branch. The long-wavelength modulational instability takes place when this pair crosses the imaginary axis. In the limit of large delay times, the distance between the imaginary parts of the neighboring eigenvalues on the pseudocontinuous branch shown in Fig. 3 becomes close to $\epsilon = 2\pi/\tau$ [35,37], the eigenvalues $\lambda_\pm$ can be expanded in power series in the small parameter ϵ as $\lambda_\pm = \pm i\epsilon[1 + \nu\epsilon/(2\pi)] + \gamma_{\pm 2}\epsilon^3/(2\pi) + \cdots$, where ν is real, since the second-order derivative along the branch vanishes at the bifurcation point. Here we used the fact that λ_- and λ_+ are complex conjugated. Substituting this expansion into the eigenvalue problem (6), representing the unknown eigenfunctions in the form $\Psi = \Psi^{\rm tr} + \epsilon\Psi_1 + \epsilon^2\Psi_{\pm 2} + \cdots$, and collecting first-order terms in ϵ we get a linear equation for the first-order correction Ψ_1:

$$L_0\Psi_1 = (I + \nu\eta B)\Psi^{\rm tr}. \tag{8}$$

Next, collecting the terms of the order ϵ^2 and applying the solvability condition to the resulting equation we obtain the third-order corrections to the real parts of $\lambda_\pm$, which lead to the following condition for the modulational instability threshold:

$$\eta_m = p^2/[2\sin\theta(qP - pQ)]. \tag{9}$$

Here the coefficients P and Q are calculated using the same formulas as those for p and q, but with $\Psi^{\rm tr}$ replaced by the first-order correction Ψ_1 obtained by solving Eq. (8). In contrast to p and q, the coefficients P and Q depend on the phase θ. The modulational instability shown with the dashed blue line in Fig. 2 gives rise to a sequence of Andronov-Hopf bifurcations taking place above the threshold defined by Eq. (9). One can see that Eq. (9) obtained in the limit of large delay provides a reasonable approximation for the

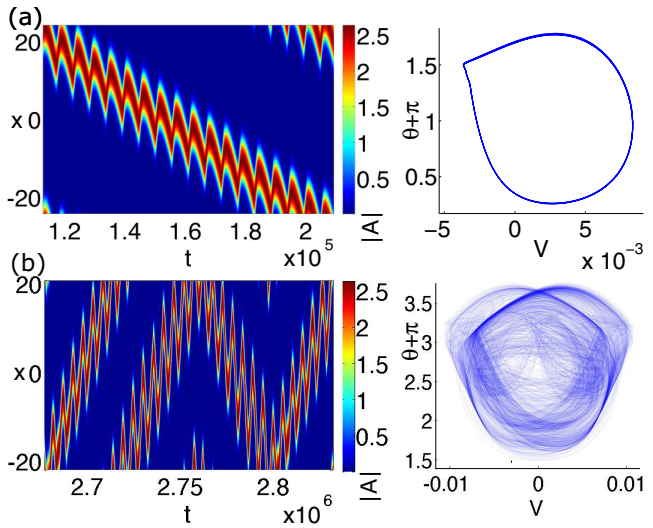

FIG. 4. Zigzagging solitons appearing above the drift and modulational instability thresholds. (a) Regime with periodic in time velocity, $\varphi = -1.0$; (b) aperiodic regime, $\varphi = 0.0$. On the right: phase portraits of zigzagging solitons in coordinates V (soliton center velocity) and θ (feedback phase). Other parameters: $\tau = 5000$, $\eta = 0.002$.

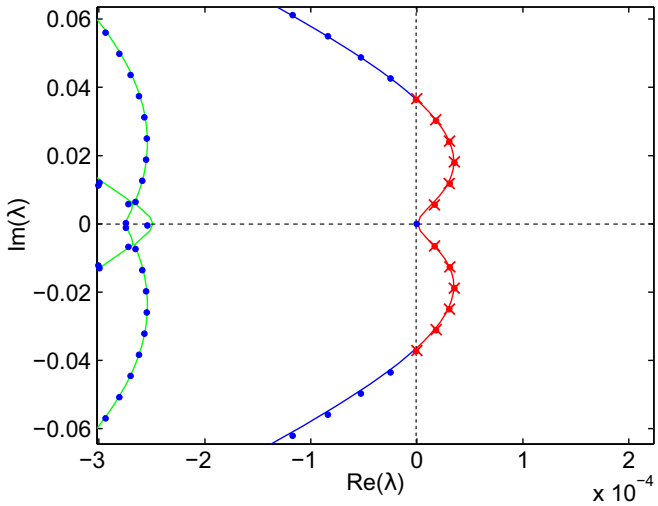

FIG. 5. Pseudocontinuous spectrum curves for $\eta = 0.09$, $\theta = 5.8$, and $\tau = 1000$. The localized solution exhibits delay-induced modulational instability of the same type as in the model of a laser with a saturable absorber. Blue dots and red crosses show stable and unstable eigenvalues for $\tau = 1000$.

Andronov-Hopf bifurcation threshold calculated at $\tau = 1000$. The latter threshold is indicated with a dotted blue line in Fig. 2.

Figure 4 shows the zigzagging motion of the soliton after the onset of both drift and modulational delay-induced instabilities. The period of oscillations is close to the delay time τ. Figure 4(a) presents a soliton with the periodically varying velocity $V_1(t)$ having a positive average value $\bar{V}_1 > 0$. It is worth noticing that a qualitatively similar zigzagging motion was observed numerically in a model of a VCSEL with frequency-selective feedback [39]. Due to the symmetry properties of the problem this periodic regime coexists with another stable periodic regime having exactly opposite velocity $V_2(t) = -V_1(t)$. With the increase of the parameter φ both periodic regimes are transformed into aperiodic solutions which finally merge into a single chaotic attractor. A period-doubling transition to chaos leads to the attractor, which corresponds to a zigzagging soliton changing the direction of motion aperiodically after large time intervals, see Fig. 4(b). Surprisingly, the time intervals between these changes of the direction of the soliton motion are much larger than the delay time or any other system time scale.

Finally, we demonstrate that the delay-induced modulational instability similar to that described above can destabilize localized solutions of the cubic-quintic complex Ginzburg-Landau equation (CGLE). CGLE plays an important role in modeling of various natural phenomena including nonlinear optical waves, second-order phase transitions, Rayleigh-Bénard convection, and superconductivity [42,43]. Its universality is ensured by the fact that CGLE is an amplitude equation describing the onset of instability near an Andronov-Hopf bifurcation in spatially extended dynamical systems [18]. In nonlinear optics, equations of the CGLE type are widely used to describe such phenomena as mode-locking in lasers [44–46], short pulse propagation in optical transmission lines [47], dynamics of multimode lasers, and transverse pattern formation in nonlinear optical media [22,48].

Here we consider one-dimensional cubic-quintic CGLE with delayed feedback. In this case the equation for the complex amplitude $A(x,t)$ reads

$$\partial_t A = \left(d + \frac{i}{2}\right)\partial_{xx} A + \delta A + (\epsilon + i)|A|^2 A + (\mu + i\nu)|A|^4 A + \eta e^{i\varphi} A(x, t - \tau). \quad (10)$$

Here the parameter $d > 0$ is the diffusion coefficient, diffraction (second-order dispersion) coefficient is scaled to $1/2$, and δ describes the linear loss or gain. Parameters ϵ, μ, and ν determine the shape of the nonlinearity.

Stable localized solutions are found in the range of parameters described in, e.g., [44]. We consider a stable localized solution for the following parameter values: $d = 0.5$, $\delta = -0.1$, $\epsilon = 0.5$, $\mu = -0.1$, and $\nu = -0.1$. With the addition of the delayed feedback, modulational instability can develop as illustrated by Fig. 5, where pseudocontinuous spectrum curves for $\eta = 0.09$, $\theta = 5.8$, and $\tau = 1000$, corresponding to modulationally unstable localized solutions, are shown.

Based on our results one can expect that the observed phenomena of delay-induced multistability as well as delay-induced modulational instability and zigzagging of localized structures appear in other spatially extended systems subject to delayed feedback.

We acknowledge the support by the German Research Foundation (DFG) in the framework of the Collaborative Research Centers SFB 910 and SFB 787, European Research Council (ERC-2010-AdG 267802, Analysis of Multiscale Systems Driven by Functionals), and Grant No. 14-41-00044 of the Russian Science Foundation, as well as the support of the Center for Nonlinear Science (CeNoS) of the University of Münster.

[1] N. N. Rosanov, *Spatial Hysteresis and Optical Patterns* (Springer, Berlin, 2002).
[2] H. Vahed, F. Prati, M. Turconi, S. Barland, and G. Tissoni, Philos. Trans. R. Soc., A **372**, 2027 (2014).
[3] M. G. Clerc, A. Petrossian, and S. Residori, Phys. Rev. E **71**, 015205 (2005).
[4] F. Arecchi, S. Boccaletti, and P. Ramazza, Phys. Rep. **318**, 1 (1999).
[5] *Dissipative Solitons: From Optics to Biology and Medicine*, Vol. 751 of Lecture Notes in Physics, edited by N. Akhmediev and A. Ankiewicz (Springer, Berlin, 2008).
[6] O. Lioubashevski, H. Arbell, and J. Fineberg, Phys. Rev. Lett. **76**, 3959 (1996).
[7] D. J. B. Lloyd, C. Gollwitzer, I. Rehberg, and R. Richter, J. Fluid Mech. **783**, 283 (2015).
[8] H. H. Rotermund, S. Jakubith, A. Von Oertzen, and G. Ertl, Phys. Rev. Lett. **66**, 3083 (1991).
[9] A. S. Mikhailov and K. Showalter, Phys. Rep. **425**, 79 (2006).
[10] H.-G. Purwins, H. U. Bödeker, and S. Amiranashvili, Adv. Phys. **59**, 485 (2010).
[11] A. W. Liehr, *Dissipative Solitons in Reaction Diffusion Systems. Mechanism, Dynamics, Interaction* (Springer, Berlin, 2013).
[12] M. Suzuki, T. Ohta, M. Mimura, and H. Sakaguchi, Phys. Rev. E **52**, 3645 (1995).
[13] S. Barland, M. Giudici, G. Tissoni, J. R. Tredicce, M. Brambilla, L. Lugiato, F. Prati, S. Barbay, R. Kuszelewicz, T. Ackemann *et al.*, Nat. Photon. **6**, 204 (2012).
[14] M. Tlidi, A. G. Vladimirov, D. Pieroux, and D. Turaev, Phys. Rev. Lett. **103**, 103904 (2009).
[15] S. V. Gurevich and R. Friedrich, Phys. Rev. Lett. **110**, 014101 (2013).
[16] A. Pimenov, A. G. Vladimirov, S. V. Gurevich, K. Panajotov, G. Huyet, and M. Tlidi, Phys. Rev. A **88**, 053830 (2013).
[17] V. V. Afanasjev, N. N. Akhmediev, and J. M. Soto-Crespo, Phys. Rev. E **53**, 1931 (1996).
[18] A. C. Newell, *Envelope Equations, Nonlinear Wave Motion*, Lectures in Applied Mathematics Vol. 15 (American Mathematical Society, Providence, RI, 1976), pp. 157–163.
[19] A. Suchkov, Zh. Eksp. Teor. Fiz. **49**, 1495 (1965) [Sov. Phys.-JETP **22**, 1026 (1966)].
[20] A. Vladimirov, N. Rozanov, S. Fedorov, and G. Khodova, Quantum Electron. **27**, 949 (1997).
[21] A. Vladimirov, N. Rozanov, S. Fedorov, and G. Khodova, Quantum Electron. **28**, 55 (1998).
[22] A. G. Vladimirov, S. V. Fedorov, N. A. Kaliteevskii, G. V. Khodova, and N. N. Rosanov, J. Opt. B: Quantum Semiclassical Opt. **1**, 101 (1999).
[23] J. Mørk, B. Tromborg, and J. Mark, IEEE J. Quantum Electron. **28**, 93 (1992).
[24] T. Heil, I. Fischer, W. Elsäßer, and A. Gavrielides, Phys. Rev. Lett. **87**, 243901 (2001).
[25] V. Rottschäfer and B. Krauskopf, Internat. J. Bifur. Chaos **17**, 1575 (2007).
[26] K. Green, B. Krauskopf, F. Marten, and D. Lenstra, SIAM J. Appl. Dyn. Syst. **8**, 222 (2009).
[27] S. Yanchuk and M. Wolfrum, SIAM J. Appl. Dyn. Syst. **9**, 519 (2010).
[28] M. C. Soriano, J. García-Ojalvo, C. R. Mirasso, and I. Fischer, Rev. Mod. Phys. **85**, 421 (2013).
[29] D. Puzyrev, S. Yanchuk, A. Vladimirov, and S. Gurevich, SIAM J. Appl. Dyn. Syst. **13**, 986 (2014).
[30] Y. Tanguy, T. Ackemann, and R. Jäger, Phys. Rev. A **74**, 053824 (2006).
[31] T. Ackemann, Y. Noblet, P. Paulau, C. McIntyre, P. Colet, W. Firth, and G.-L. Oppo, in *Spontaneous Symmetry Breaking, Self-Trapping, and Josephson Oscillations*, edited by B. A. Malomed, Vol. 1 of Progress in Optical Science and Photonics (Springer, Berlin, 2013), pp. 49–87.
[32] Z. Wu and W. Michiels, J. Comp. Appl. Math. **236**, 2499 (2012).
[33] G. Iooss and D. Joseph, *Elementary Stability and Bifurcation Theory* (Springer, New York, 2013).
[34] Note that the same relation (7) can be obtained from the orthogonality condition of the generalized eigenfunction $\Phi^{\rm tr}$, which satisfies the equation $L_0\Phi^{\rm tr} = \Psi^{\rm tr}$, and the adjoint neutral mode $\Psi^{\rm tr\dagger}$ with the bilinear form defined in [40,41].
[35] M. Lichtner, M. Wolfrum, and S. Yanchuk, SIAM J. Math. Anal. **43**, 788 (2011).
[36] S. Heiligenthal, T. Dahms, S. Yanchuk, T. Jüngling, V. Flunkert, I. Kanter, E. Schöll, and W. Kinzel, Phys. Rev. Lett. **107**, 234102 (2011).
[37] J. Sieber, M. Wolfrum, M. Lichtner, and S. Yanchuk, Discrete Contin. Dyn. Syst. A **33**, 3109 (2013).
[38] M. Wolfrum, S. Yanchuk, P. Hövel, and E. Schöll, Eur. Phys. J. ST **191**, 91 (2010).
[39] P. V. Paulau, D. Gomila, P. Colet, M. A. Matías, N. A. Loiko, and W. J. Firth, Phys. Rev. A **80**, 023808 (2009).
[40] S. Guo and J. Wu, *Bifurcation Theory of Functional Differential Equations*, Applied Mathematical Sciences (Springer, New York, 2013).
[41] A. Luo and J. Sun, *Complex Systems: Fractionality, Time-delay and Synchronization*, Nonlinear Physical Science (Springer, Berlin, 2011).
[42] M. C. Cross and P. C. Hohenberg, Rev. Mod. Phys. **65**, 851 (1993).
[43] I. S. Aranson and L. Kramer, Rev. Mod. Phys. **74**, 99 (2002).
[44] J. M. Soto-Crespo, N. Akhmediev, and V. V. Afanasjev, J. Opt. Soc. Am. B **13**, 1439 (1996).
[45] N. Akhmediev, A. Ankiewicz, and J. M. Soto-Crespo, J. Opt. Soc. America B **15**, 515 (1998).
[46] P. Grelu and N. Akhmediev, Opt. Express **12**, 3184 (2004).
[47] M. Matsumoto, H. Ikeda, T. Uda, and A. Hasegawa, J. Lightwave Technol. **13**, 658 (1995).
[48] K. Staliunas, R. Herrero, and G. J. de Valcárcel, Phys. Rev. A **75**, 011604(R) (2007).